Journal of Research and Applications in Mechanical Engineering
ISSN: 2229-2152 (Print); 2697-424x (Online)
(2026) Vol. 14, No. 1, Paper No. JRAME 26-14-007
[DOI: 10.14456/ jrame.2026.7]

Research Article

Effect Triangular Baffles on Thermal- Hydraulic Optimization and Turbulent Flow CuO/ Water Nanofluid in 2D Channel Using Computational Fluid Dynamics Method

S.A. Ali[1,*]
A.M. Ashour[2]
M.R. Hameed[1]
[1] *Department of Automobile Engineering, College of Engineering–Al Musayab, University of Babylon, Babylon, 51001, Iraq.*
[2] *Department of Mechanical Engineering, Faculty of Engineering, University of Technology, Baghdad, 10001, Iraq.*

Received 27 December 2024
Revised 17 February 2025
Accepted 20 February 2025

Abstract:
In large-scale applications, fluid flow with baffles is a multifaceted phenomenon because it plays an important role in improving heat transfer and mixing in addition to other fluid dynamics processes. To achieve the required heat transfer, the design of triangular baffle models inside the channel is of great importance. In the present work, the effect of the inclusion of baffles in the upper and lower surface of a two-dimensional channel of a nanofluid flow (CuO+Water) with volumetric fractions (5%) steady-state single-phase turbulence with Reynolds number ranges of (7000-17000) is numerically studied. The channel is divided into three main sections, the first and the last are thermally insulated, and the second is subjected to a constant uniform heat flux of (30 kW/m^2). Using the finite volume method of the Ansys Fluent program, all the equations governing the fluid flow inside the channel, including the conservation of mass, momentum, and heat energy, were solved using the turbulent k-ε for high Reynolds values. The numerical results of the current study indicated that the heat transfer rate gradually increases with an increase in the Reynolds number, while the friction factor gradually decreases with an increase in the Reynolds number, moreover, the values of the Nusselt number and the friction factor were affected by the height of the baffles, where the increase in height both increases gradually, it was also found that the height of (12 mm) gave the highest percentage of heat transfer enhancement with a value of (82.69%) compared to the other heights (2, 4, 6, 8 and 10 mm), which gave a ratio of (60.46, 70.01 and 80.65%), respectively. Finally, the pressure, temperature and velocity distribution of the nanofluid differed when the baffles were placed to disturb the passing flow compared to the normal empty channel.

Keywords: *Triangular Baffles, Numerical Simulation, Forced Convection, Channel, Fluid Flow, Nanoparticles*

1. Introduction

Contributing to raising the efficiency of thermal devices for various engineering applications is an important research area because it results from increasing and improving heat transfer. Without reducing the overall efficiency of these devices to increase heat transfer, passive methods are used for various configurations, including vortex generators, corrugated channel geometry, channel baffles, fins and ailerons.

* Corresponding author: S.A. Ali
E-mail address: sarmad.ahmed96@uobabylon.edu.iq

Engineering industrial applications include nuclear reactors, transportation, air conditioning systems, refrigeration, solar air heaters, heat exchangers, as well as food or chemical processing. Compared to other technologies, this method is considered reliable and economical because it does not require external energy and also does not involve dynamic movement [1-8]. To improve the thermal-hydraulic performance in the petrochemical, biomedical, chemical, biological and other industries, specifically the heat exchangers widely used in those industries, one of the passive improvement techniques is used, including baffles. The working fluid is directed from the side of the casing to move back and forth through the inner tube, which leads to increased turbulence while providing a good mixing of fluid layers in addition to eliminating dead spots, this is the reason why baffles are often used in heat exchangers and channels to increase the heat transfer rate [9 and 10]. Suvanjan Bhattacharyya et al. [11] presented a numerical study to analyze the properties of heat transfer and laminar flow with low Reynolds numbers in a small corrugated microchannel of the upper wall in the presence of an external magnetic field. Recent studies have proven that corrugated walls give the best heat transfer compared to straight walls. Laminar flow was used because it gives less energy consumption compared to turbulent flow. The basic fluid (water) was mixed with nanoparticles of fractional size (2%) under the influence of a magnetic field to generate the nanofluid. Pranita Bichkar et al. [12] studied numerically using a simulation program by including three different types of baffles, including single, double and spiral sectional, to show their effect on the pressure drop of the heat exchanger tube. The formation of dead zones appears using single sectional baffles in which heat transfer is ineffective, while vibrational damage is significantly reduced when using double sectional baffles, moreover, dead zones disappear using spiral sectional baffles, which produces a good effective heat transfer. Younes Menni et al. [13] presented a numerical characterization and investigation of the mass transport of heat and (Al_2O_3+H_2O) nanofluid across a two-dimensional conduit with connected and removed baffle plates. Using the energy equation and the typical k-epsilon turbulence model, the Reynolds-averaged Navier-Stokes equations control the physical component. This study employs the Finite Volume Method using the Semi Implicit Method for Pressure Linked Equations (SIMPLE) method and the Quadratic Upstream Interpolation for Convective Kinetics (Quick) numerical scheme using the commercial computational fluid dynamics program (ANSYS FLUENT). M. Nithya et al. [14] presented a research study on the impact of the introduction of baffles on the performance of the heat exchanger, namely heat transfer, pressure drop and fluid flow characteristics. To obtain the optimal configuration of baffles Computational Fluid Dynamics was used. To get the calculation algorithm working correctly, a detailed study was carried out to validate the results, including the turbulence model and the number of optimal mesh. The findings indicate that the wedge and aerofoil types' Performance Evaluation Criterion is around 1.24 to 1.3 and 1.22 to 1.24, respectively, in comparison to the conventional one. Selma Akçay [15] studied a numerical simulation using the finite volume method to demonstrate the effect of Central ailerons with a flow of nanofluid (Al2O3 + Water) inside a corrugated channel. Using a simple algorithm, Computational Fluid Dynamics-based analyses are performed within low Reynolds numbers for ranges (200-1200). The fractional sizes of nanomaterials vary by ranges (1-5%). A constant temperature of (350K) is applied to the upper and lower surfaces. At different Reynolds number numbers, the velocity and temperature distribution of the winding channel with and without ailerons is obtained. The results of the study indicated the inclusion of nanofluid with ailerons in the corrugated channel significantly contributes to enhancing heat transfer, but the friction factor increases compared to the empty channel. In addition, the heat transfer represented by the Nusselt number increases with increasing fluid flow velocity and the ratio of volumetric fractions. Dipankar De et al. [16] presented a numerical investigation of improving the heat transfer rate and flow characteristics using helical-type baffles in a heat exchanger for comparison against straight-type baffles. The Ansys program was used as a simulation tool, while all the model designs are by CATIA software. Seven copper tubes, each measuring 20 mm in external diameter and 17 mm in internal diameter, are included in the model. They are 600 mm long, with an inner diameter of 90 mm and an outside diameter of 110 mm for the steel shell. Six straight or helical aluminum baffles, with helix angles ranging from 0 to 30 degrees, retain seven tubes. T. Lima-Téllez et al. [17] numerically indicated the study of the effect of different types of nanomaterials (Al_2O_3, ZnO and CuO) on the thermo-hydraulic performance of the solar PV panel system. To simulate the interaction between the fluid in motion and the plate material the method of Computational Fluid Dynamics was used. The concentrations of different nanoparticles were examined at the ranges and values of solar radiation and Reynolds numbers (0 .2 -1 kW/m^2) (18-1800), respectively. At the lowest Reynolds number range, the numerical results showed the CuO-type nanofluid improved thermal efficiency by 5.67% compared to other types. P. Nithish Reddy et al. [18] using the finite volume method numerically studied under different operating conditions and design parameters evaluate, understand and visualize the inclusion of baffles inside the channel on heat transfer rates with Reynolds number range (1800-22000). For various engineering configurations to check the thermal performance of the channels, Computational Fluid Dynamics investigations were carried out, including baffles with the shape (V), circular and triangular. A V-shaped baffle case has a higher friction factor even if its thermal performance is generally good. Ali, Sarmad A. and Suhad A. Rasheed. [19] presented a numerical analysis of the

optimization of forced convection heat transfer and laminar flow characteristics in a two-dimensional horizontal channel with a square cross-section (12 x12 cm). A uniform constant heat flux with a value of (1500 W/m^2) was projected onto the surface of the upper and lower walls of the channel towards the flow axis. The improvement process included the inclusion of a porous medium inside the channel to increase heat transfer, as well as studying the effect of changing the angle (0°, 15°, 30° and 45°) test model on the distribution of temperature, pressure and speed. The numerical results showed that the Nusselt number increases gradually by increasing the Reynolds number while the friction factor decreases gradually, moreover, the Nusselt number values increased using the porous medium compared to the empty channel. Ali SA et al. [20] touched upon the inclusion of various shapes of square, circular, and triangular dimples in a three-dimensional turbulent flow tube at a Reynolds number range (3500-7000) to enhance the thermal performance of the heat exchanger tube. The flow-governing equations of continuity, momentum and thermal energy have been solved numerically. The results indicated the dimples improved heat transfer compared to the smooth tube, where the best improvement is when using the round shape among other shapes.

The current work focuses on the enhancement of heat transfer by forced convection with turbulent nanofluid flow (CuO with water) in Reynolds number ranges of (7000-17000) in a two-dimensional channel inserted inside baffles with triangular configurations as a means of optimization. The effect of several parameters on the hydrothermal performance, including the height (4, 6, 8, 10 and 12 mm) and Reynolds number, was numerically analyzed using the Ansys fluent software based on the finite volume method (FVM). The use of combined methods to improve the flow properties with increased heat transfer by nanomaterials and baffles obstructing the flow is the research gap of the current study, as many previous studies deal with enhancing heat transfer using a single method.

2. Mathematical of Numerical Model

2.1 Description of Physical Problem

Figure (1) highlights the basic geometry of the two-dimensional channel of the current numerical study. The channel is two parallel boards with a length and height (0.5 and 0.02 m), respectively. Three main sections of the channel consist of an adiabatic section with a length of (0.3 m), a hot section with a length of (0.17 m) and another adiabatic section with a length of (0.03 m). Two baffles for better heat transfer were installed inside the channel and one on the upper wall at different distances (0.03, 0.05, 0.07, 0.09 and 0.12 m) towards the axis of the flow of the other fluid on the lower wall by a distance of (0.015 m). The dimensions of the baffles used are equal for both with different heights (0.004, 0.006, 0.008, 0.01 and 0.012 m) with a fixed width (0.008 m). The upper and lower walls of the heated channel have a uniform constant heat flux of (30 kW/m^2). The hypotheses of the study are single-phase steady-state turbulent flow with a Reynolds number range (7000-17000). The homogeneous mixture consists of water with spherical nanoparticles (CuO).

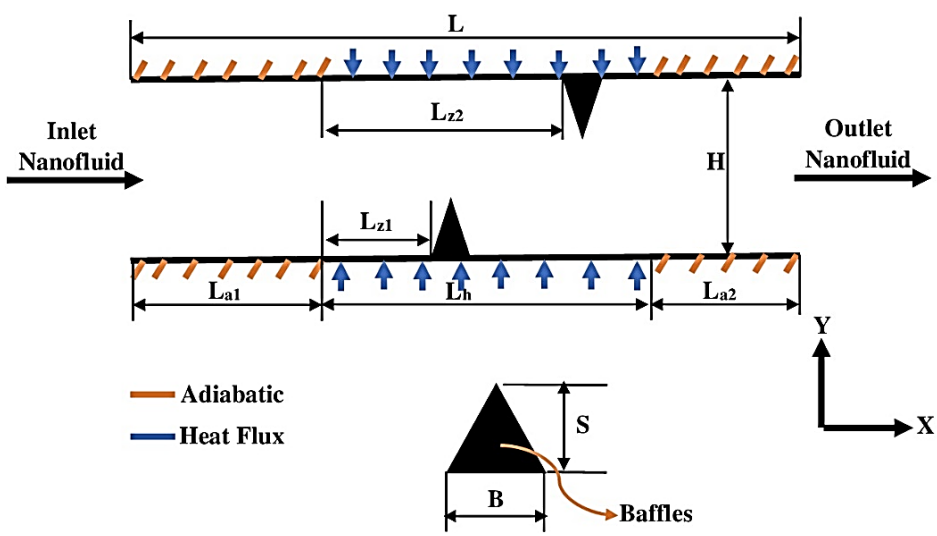

Fig. 1. Physical model of current study with triangular baffles.

2.2 Thermal-physical characteristics of CuO/ Water Nanofluid

All thermophysical properties related to the basic fluid (water) and nanoparticles represented by calcium oxide (CuO), as well as the properties of the nanomaterial (CuO+ Water) at a volumetric fraction (5%) are listed in Tables (1 and 2), respectively.

Table 1: Thermophysical properties for working fluid and nanoparticles at (298 K) [21 and 22].

Properties	Unit	Water	CuO
ρ	$kg.m^{-3}$	997	6400
Cp	$J.kg^{-1}. K^{-1}$	4180	535.6
λ	$W.m^{-1}. K^{-1}$	0.607	76.5
μ	$Pa. s^{-1}$	0.000891	-------

The thermophysical properties of the nanomaterial are calculated according to the following mathematical equations [23-26]:

The calculation of the density of a nanomaterial is:

$$\rho_{nf} = (1-\varnothing)\rho_{bf} - \varnothing\rho_{np} \tag{1}$$

The heat capacity of a nanomaterial is calculated by:

$$Cp_{nf} = (1-\varnothing)Cp_{bf} - \varnothing Cp_{np} \tag{2}$$

Finding the thermal conductivity of nanomaterials from:

$$\lambda_{nf} = \frac{\lambda_{bf} + \lambda_{np} + 2\lambda_{bf} - 2\varnothing(\lambda_{bf} - \lambda_{np})}{\lambda_{np} + 2\lambda_{bf} + \varnothing(\lambda_{bf} - \lambda_{np})} \tag{3}$$

The definition of the viscosity of a nanomaterial is:

$$\mu_{nf} = \mu_{bf}(123\varnothing^2 + 7.3\varnothing + 1) \tag{4}$$

Table 2: Thermophysical properties of nanofluid.

Ø	ρ ($kg.m^{-3}$)	Cp ($J.kg^{-1}. K^{-1}$)	λ ($W.m^{-1}. K^{-1}$)	μ ($Pa. s^{-1}$)
5 %	627.15	3944.22	1.1622	0.00149

2.3 Flow Governing Equations and Boundary Conditions

The governing equations of forced heat flow inside the channel for a two-dimensional turbulent nanofluid can be written in Cartesian form according to the following [27-30]:

The continuity equation is:

$$\frac{\partial}{\partial x}(\rho u) + \frac{\partial}{\partial y}(\rho v) = 0 \tag{5}$$

The momentum equation in the X-direction is:

$$\frac{\partial}{\partial x}(\rho uu) + \frac{\partial}{\partial y}(\rho uv) = \frac{-\partial p}{\partial x} + \frac{\partial}{\partial x}[(\mu+\mu_t)\frac{\partial u}{\partial x}] + \frac{\partial}{\partial y}[(\mu+\mu_t)\frac{\partial u}{\partial y}]$$
$$+ \frac{\partial}{\partial x}[(\mu+\mu_t)\frac{\partial u}{\partial x} - \frac{2}{3}\rho\lambda] + \frac{\partial}{\partial y}[(\mu+\mu_t)\frac{\partial v}{\partial x}] \tag{6}$$

The momentum equation in Y-direction is:

$$\frac{\partial}{\partial x}(\rho uv)+\frac{\partial}{\partial y}(\rho vv)=\frac{-\partial p}{\partial y}+\frac{\partial}{\partial x}[(\mu+\mu_t)\frac{\partial v}{\partial x}]+\frac{\partial}{\partial y}[(\mu+\mu_t)\frac{\partial v}{\partial y}]$$
$$+\frac{\partial}{\partial y}[(\mu+\mu_t)\frac{\partial v}{\partial y}-\frac{2}{3}\rho\lambda]+\frac{\partial}{\partial x}[(\mu+\mu_t)\frac{\partial u}{\partial y}] \quad (7)$$

The heat energy equation is:

$$\frac{\partial}{\partial x}(\rho uT)+\frac{\partial}{\partial y}(\rho vT)=\frac{\partial}{\partial x}[(\frac{K}{Cp}+\frac{\mu_t}{\mathrm{Pr}_t})\frac{\partial T}{\partial x}]+\frac{\partial}{\partial y}[(\frac{K}{Cp}+\frac{\mu_t}{\mathrm{Pr}_t})\frac{\partial T}{\partial y}] \quad (8)$$

This work estimates the turbulent dynamic viscosity using the Launder-Sharma k-ε model. These models are described as [31]:

The calculation of the equation of turbulent kinetic energy (k) is:

$$\frac{\partial}{\partial x}(\rho uk)+\frac{\partial}{\partial y}(\rho vk)=\frac{\partial}{\partial x}[\Gamma_k\frac{\partial k}{\partial x}]+\frac{\partial}{\partial y}[\Gamma_k\frac{\partial k}{\partial y}]+P_k-\rho(\varepsilon-\varepsilon_w) \quad (9)$$

Where ε is the dissipation rate in the wall can be expressed as follows:

$$\varepsilon_w=2\frac{\mu}{\rho}[(\frac{\partial\sqrt{k}}{\partial x})^2+(\frac{\partial\sqrt{k}}{\partial y})^2] \quad (10)$$

The equation of dissipation turbulence kinetic energy (ε) is:

$$\frac{\partial}{\partial x}(\rho u\varepsilon)+\frac{\partial}{\partial y}(\rho v\varepsilon)=\frac{\partial}{\partial x}[\Gamma_\varepsilon\frac{\partial\varepsilon}{\partial x}]+\frac{\partial}{\partial y}[\Gamma_\varepsilon\frac{\partial\varepsilon}{\partial y}]+(C_1f_1P_k-\rho C_2f_2\varepsilon)\frac{\varepsilon}{k}+\phi_\varepsilon \quad (11)$$

where;

$$\phi_\varepsilon=2\mu_t\frac{\mu}{\rho}[(\frac{\partial^2u}{\partial x^2})^2+(\frac{\partial^2v}{\partial x^2})^2+2(\frac{\partial^2u}{\partial x\partial y})^2+2(\frac{\partial^2v}{\partial x\partial y})^2+(\frac{\partial^2u}{\partial y^2})^2+(\frac{\partial^2v}{\partial y^2})^2] \quad (12)$$

The equation of turbulence kinetic energy production rate is calculated from:

$$P_k=\mu_t\{2[(\frac{\partial u}{\partial x})^2+(\frac{\partial v}{\partial y})^2]+(\frac{\partial u}{\partial y}+\frac{\partial v}{\partial x})^2)^2\}-\frac{2}{3}\rho k(\frac{\partial u}{\partial x}+\frac{\partial v}{\partial y}) \quad (13)$$

The turbulent viscosity can be calculated from the following relation:

$$\mu_t=C_\mu f_\mu\rho\frac{k^2}{\varepsilon} \quad (14)$$

The perturbative Prandtl number and the empirical constants can be expressed as follows:

$$C_\mu=0.09, C_1=1.44, C_2=1.92, \sigma_k=1.0, \sigma_\varepsilon=1.3, \mathrm{Pr}=0.9$$

According to the following the wall damping functions were expressed as well as the perturbed Reynolds number [32]:

$$f_1=1.0 \quad (15)$$

$$f_2=1=0.3\exp(-\mathrm{Re}_T^2) \quad (16)$$

$$f = \exp[-3.4/(1+0.02\,\mathrm{Re}_T)^2] \tag{17}$$

$$\mathrm{Re}_T = \frac{\rho}{\varepsilon}\frac{k^2}{\mu} \tag{18}$$

The boundary conditions corresponding to the two-dimensional channel expressed are as follows [33]:

- At the portion of the inlet:

$$u = u_{in}, v = 0, T = T_{in}, k = k_{in} = \frac{2}{3}(I_o u_{in})^2, \varepsilon = C\mu^{\frac{3}{4}} k_{in}^{\frac{3}{2}} / (0.07 D_h) \tag{19}$$

- At the portion of the outlet:

$$\frac{\partial u}{\partial x} = 0, \frac{\partial v}{\partial x} = 0, \frac{\partial T}{\partial x} = 0, \frac{\partial k}{\partial x} = 0, \frac{\partial \varepsilon}{\partial x} = 0 \tag{20}$$

Along the total length of the channel walls:

$$u = 0, v = 0, k = 0, \varepsilon = 0 \tag{21}$$

$$\left.\frac{\partial T}{\partial y}\right|_w = \frac{-q_w}{k_{eff}} \qquad \text{For the heated wall} \tag{22}$$

$$\left.\frac{\partial T}{\partial y}\right|_w = 0 \qquad \text{For the adiabatic wall} \tag{23}$$

The properties of the thermal field/flow are obtained after solving the governing mathematical equations because they are used to determine the local and average Nusselt number, the local skin friction factor, the friction factor as well and the hydraulic thermal performance factor [34]. The following equation is used to calculate the local Nusselt number:

$$Nu_x = \frac{D_h}{\lambda_{eff}}\frac{q_w}{(T_w - T_b)} \tag{24}$$

The fluid bulk temperature can be calculated from the following equation:

$$T_b = \frac{\iint_A \rho u C p T dA}{\iint_A \rho u C p dA} \tag{25}$$

By integrating the local Nusselt number along the axis of the channel wall, the average Nusselt number can be evaluated as follows:

$$Nu_{ave} = \frac{1}{L_h}\int_{L_{a1}}^{L_{a1}+L_h} Nu_x dx \tag{26}$$

The thermal performance factor and the friction factor can be defined according to the following equations, respectively [35]:

$$TPF = \frac{\left(Nu_{av}/Nu_{av,o}\right)}{(f/f_o)^{1/3}} \tag{27}$$

$$f = \frac{2\Delta p D_h}{L\rho_{nf} u_{in}^2} \tag{28}$$

3. Numerical Solution of Computational Model

To perform the numerical solution in the current work, the Computational Fluid Dynamics code was developed based on the Fortran language (90). Using the finite volume method, the flow governing equations with appropriate boundary conditions were estimated to achieve the coupling between velocity and pressure, a simple algorithm was used [36]. The downwind plot is used in the governing equations to estimate convection terms, while the second-order central divergence plot is used to estimate diffusion terms. Moreover, the development of the computational mesh is carried out by solving Poisson's equations. Additionally, a collocated grid structure has been used to store all of the physical variables at the same nodes of the computational mesh [37]. To achieve the best numerical convergence on all physical variables, a low relaxation is applied, so with a limit of (10^{-6}) for each variable, the convergence is set as shown in Figure (2).

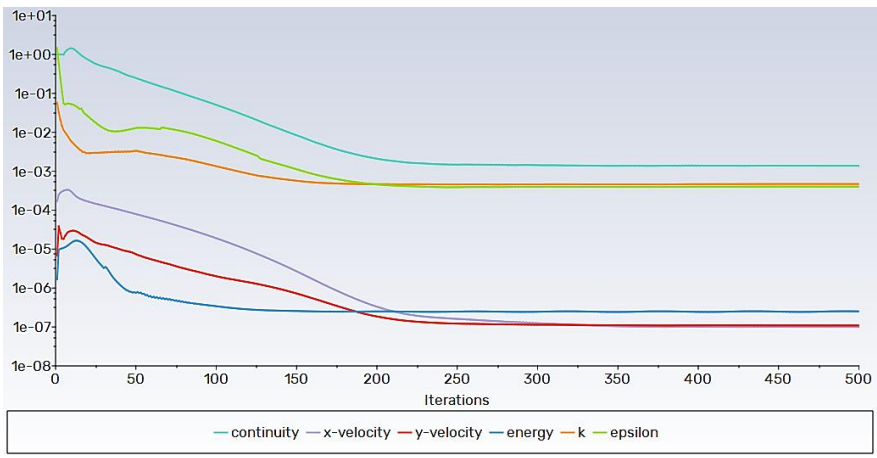

Fig. 2. Numerical convergence of the governing equations in the computational model.

4. Numerical Mesh Independence Test

The use of small cell sizes to set the optimization of the numerical results of the model is what is known as mesh independence as shown in Figure (3). The correct result should be obtained by numerical calculation for a mesh of extremely small size. In a coarse grid with which the ordinary CFD technique begins and gradually improves, the detected numerical values become small. This is problematic in two ways. First of all, using alternative CFD software to gain even in a single coarse mesh can be quite challenging, leading to various issues. Second, it may take longer to refine a mesh by a factor of two or more. For software meant to be utilized as an engineering tool with limited production capabilities, this is disrespectful. Furthermore, the other problems have greatly contributed to the idea that CFD is a very challenging, expensive and time-consuming approach. Finally, to achieve the network independence of the computational model in each case the Nusselt number was recorded and sequenced. Figure (4) shows the generation and selection of the appropriate grid type on the surface of the empty tube and the tube supported by triangular barriers, where the edges of the surface were divided into very small pieces to achieve accuracy in numerical results and numerical convergence. Choosing the right grid plays an important and effective role in the process of improving heat transfer and numerical results.

5. Results and Discussions

A numerical study investigates the effectiveness of changing the height of baffles with triangular configurations in enhancing the rate of heat transfer by forced convection with turbulent nanofluid flow inside the two-dimensional channel. This section will deal with the analysis and discussion of the results of current physical problems. Figures (5, 6 and 7) show, respectively, the pressure, temperature and velocity distribution of the nanofluid flow inside the horizontal channel at Reynolds (11000) by changing the height of the triangular baffles with values of (4, 6, 8, 10 and 12 mm) for comparison against the empty channel. It can be observed that the pressure value at entry is recorded higher, after which it gradually decreases to the outlet, while in the presence of baffles, there is a high value up to the thermal overflow zone as a result of the collision of the nanofluid with the listed baffles obstructing the flow, after

which it also decreases with increasing height, the amount of pressure at entry increases and decreases at the outlet. The temperature distribution without baffles increases as the fluid flows along the flow axis, when baffles are inserted and the height changes, the percentage of increase with temperature distribution increases. In a normal channel, the velocity of the nanofluid registers the highest value in the middle and decreases down to the surface of the channel wall, while with the inclusion of baffles, a change in the velocity gradient was observed as a result of obstruction and turbulence of the fluid, where the highest value of the velocity appeared at the distance separating the upper and lower baffles, moreover, by increasing the height, the passage of the nanofluid between the baffles decreases and slows down, therefore the shape of the contiguous layer changes.

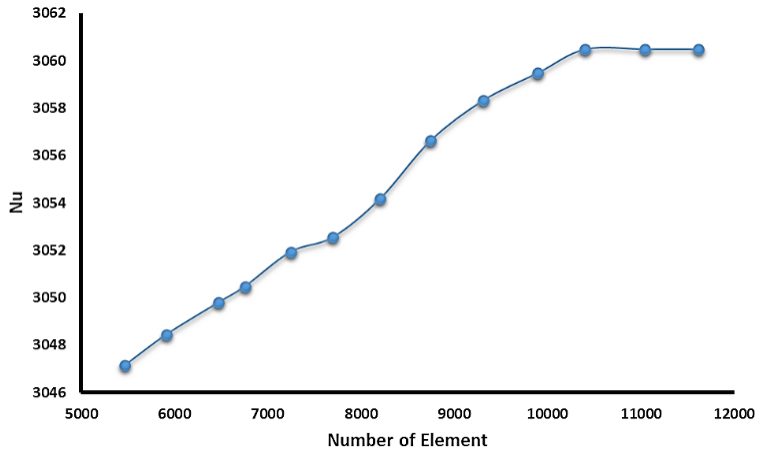

Fig. 3. Test of mesh independence for the numerical model.

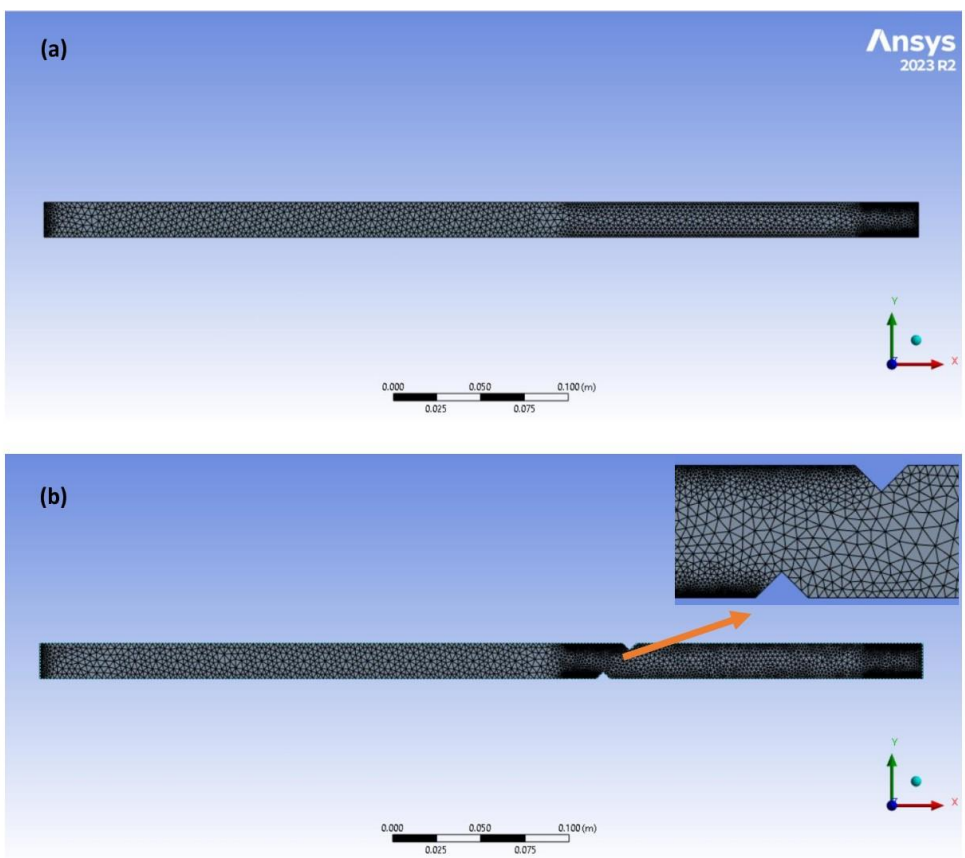

Fig. 4. Generation mesh of numerical model: (a) smooth pipe without baffles (b) pipe with triangular baffles.

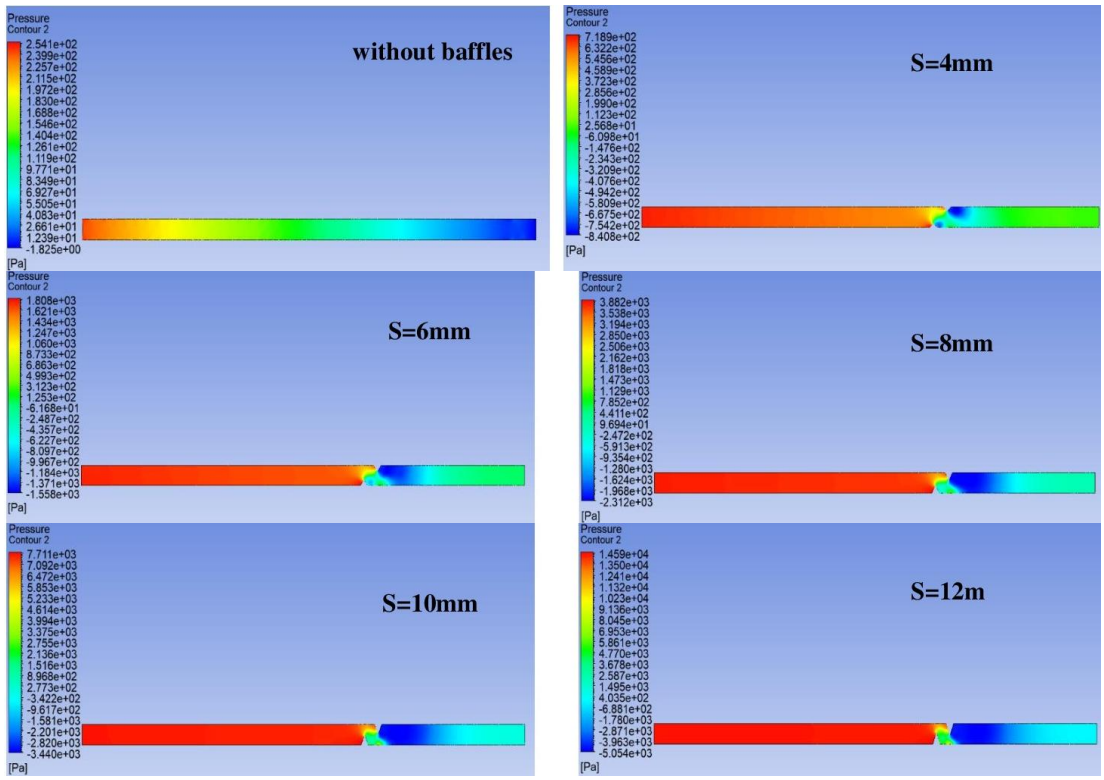

Fig. 5. Contour pressure of computational model without/ with different height triangular baffles at Re of (11000).

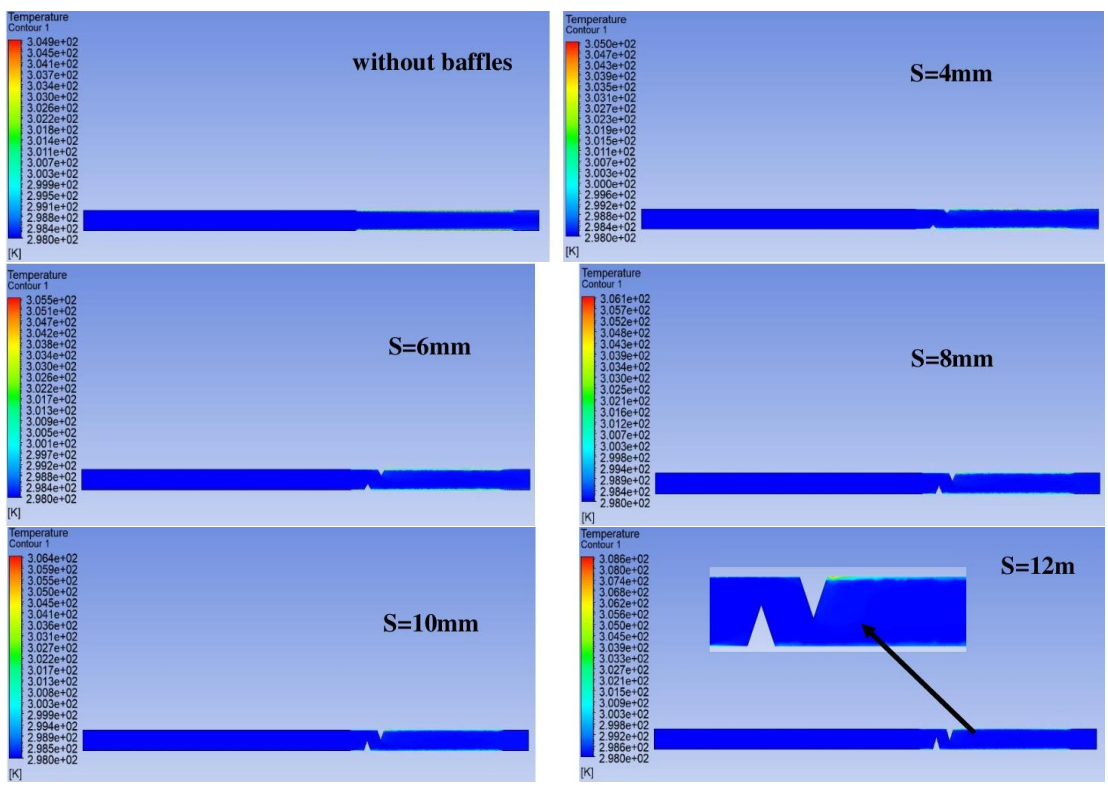

Fig. 6. Contour temperature of a computational model without/ with different height triangular baffles at Re of (11000).

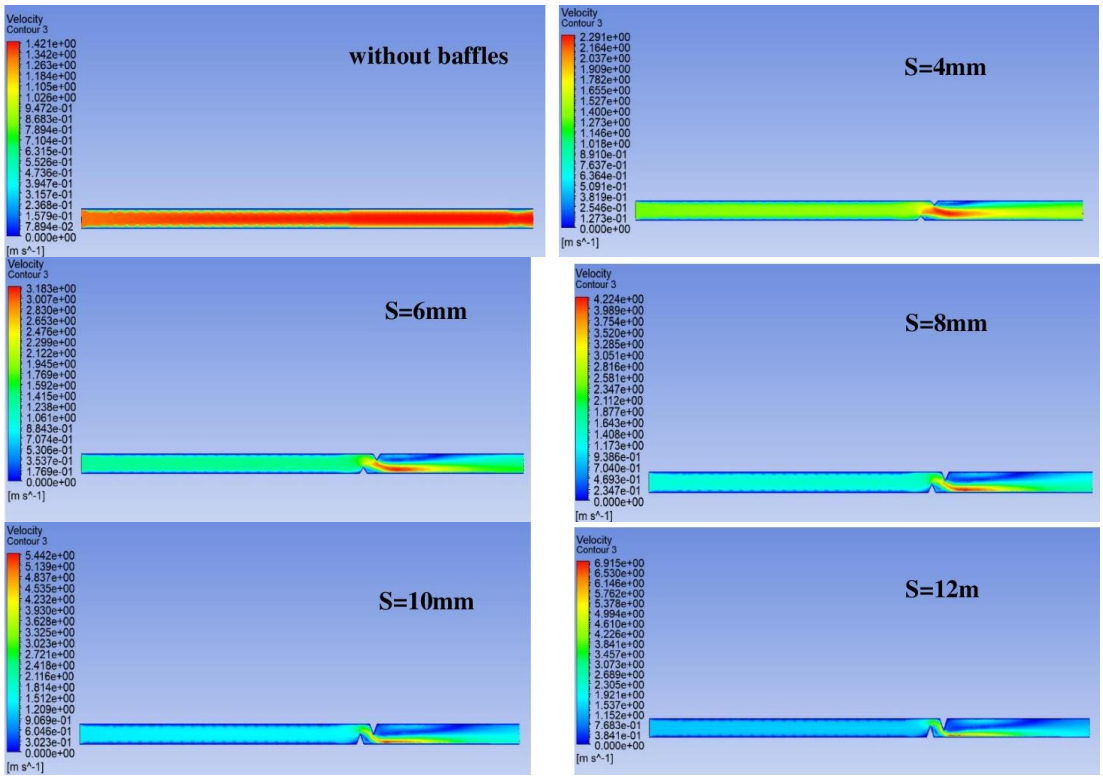

Fig. 7. Contour velocity of a computational model without/ with different height triangular baffles at Re of (11000).

Figure (8) indicates the change of the heat transfer rate represented by the Nusselt number against the Reynolds number at different scales of the turbulent nanofluid flow. The increase in the number of Nusselt can be observed gradually by increasing the Reynolds number to continue increasing the height of the triangular baffles included in the upper and lower surfaces of the channel, moreover, the number of Nusselt increases by a percentage (60.46, 70.01, 80.65 and 82.69 %) at a height of (4, 6, 8,10 and 12) respectively, compared to the normal empty channel. It found that the height at a value of (12 mm) gave the best enhancement of heat transfer compared to other heights, this happened as a result of good mixing of the nanofluid passing inside the horizontal channel.

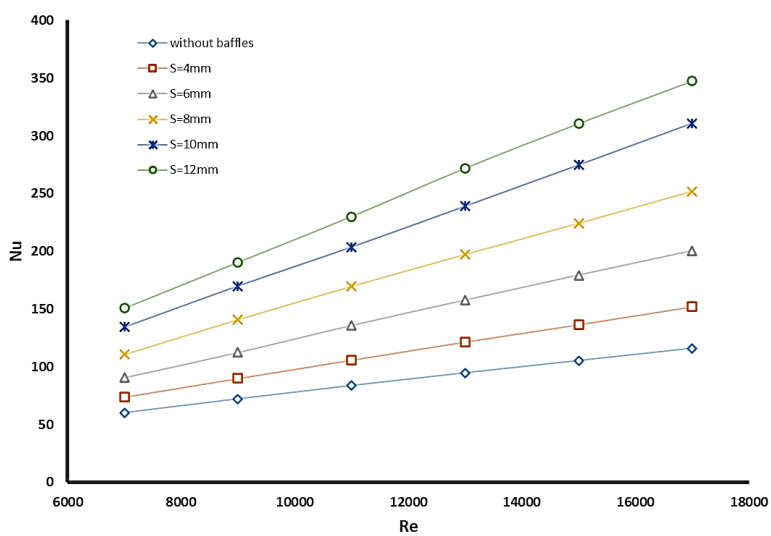

Fig. 8. Variation of Nusselt number with Reynolds number at different channel triangular baffles height.

By increasing the Reynolds number, the friction factor gradually decreases to show a change in values, as shown in Figure (9). The noticeable effect of the baffles of triangular configuration can be observed with the walls of the upper and lower surfaces of the channel. It was found that with an increase in height, the friction factor increases compared to the flow of the nanofluid in the empty channel, this happens as a result of the turbulence of the passing fluid colliding with the baffles, where the higher the height, the higher the values of the friction factor were recorded, which is considered a negative phenomenon for the use of baffles.

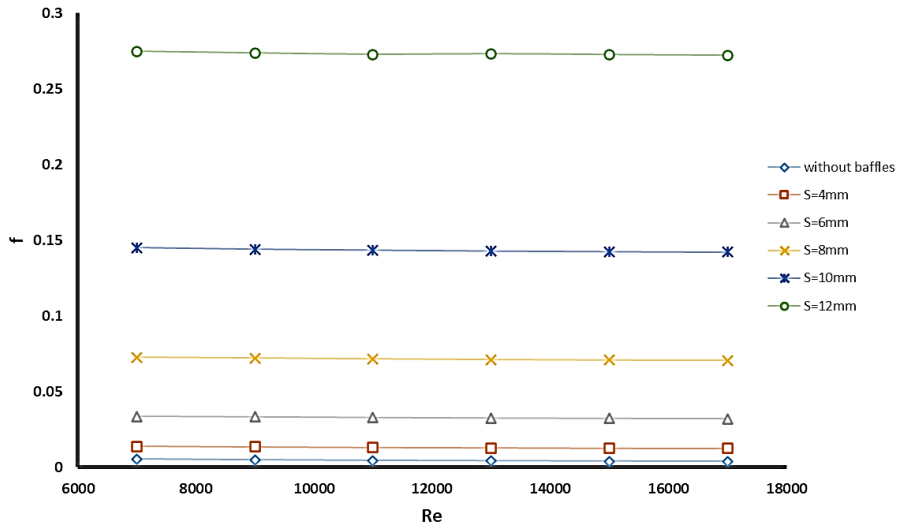

Fig. 9. Variation of friction factor with Reynolds number at different channel triangular baffles height.

6. Conclusions

The present paper deals with a numerical study using the Ansys Fluent program based on the finite volume method to achieve thermal properties of nanofluid (CuO/Water) with volume fractions of (5%) with turbulent single-phase internal flow at Reynolds number ranges of (7000-17000). All the governing equations (continuity, momentum, and heat energy) are solved numerically using the (k-ε) turbulence model. The influence of flow and geometric parameters (height of baffles) on the thermophysical properties and the thermal field were considered. The results of the study showed that the heat transfer rate improves when including baffles that cause flow obstruction compared to the smooth channel, where it was found that the height of (12mm) recorded the highest rate of heat transfer enhancement by (82.69%) Also the friction factor decreases gradually with an increase in the number of Reynolds and increases with the increase in the height of triangular baffles. The baffles adhering to the surfaces of the upper and lower walls of the channel caused a change in the shape of the boundary layer, therefore, the distribution of pressure, temperature, and velocity completely changed compared to the normal empty channel.

Nomenclature

B	Width of triangular baffle (m)
Cp	Specific heat at constant pressure (J/kg. K)
D	Channel Diameter (m)
f	Dimensionless friction factor
H	Total channel height (m)
h	Coefficient of heat transfer (W/m^2. K)
k	Turbulence kinetic energy (m^2/s^3)
L	Total channel length (m)
La_1 and La_2	Adiabatic length of parts one and two, respectively (m)
L_h	Total heated channel (m)
L_{z1} and L_{z2}	The distance between the heating start of the baffle site of the upper and lower wall respectively (m)
Nu	Dimensionless Nusselt number

p	Fluid pressure (N/m^2)
Pr	Dimensionless Prandtl number
Re	Dimensionless Reynolds number
S	Height of triangular baffle (m)
TPF	Thermal Performance Factor
X and Y	Cartesian two-dimensional channel (m)
Δp	Channel pressure drop (N/m^2)
μ	Working fluid dynamic viscosity (Pa. s)
Ø	Nanoparticle volume fraction (%)
ε	Dissipation rate of turbulence model (m^2/s^3)
λ	Working fluid thermal conductivity (W/m. K)
ρ	Working fluid density (kg/m^3)
σ	Turbulent model constant
Subscript	
ave	Average
b	Bulk
bf	Base fluid
eff	Effective
h	Hydraulic
in	inlet
nf	Nanofluid
np	nanoparticle
o	Without
t	Turbulence
w	Wall

References

[1] Zhu Z, Zhang M. Water vapor adsorption on desiccant materials for rotor desiccant air conditioning systems. Processes. 2023;11(7):2166.

[2] Chen Q, Jones JR, Archer RH. A dehumidification process with cascading desiccant wheels to produce air with dew point below 0 °C. Applied Thermal Engineering. 2019;148:78–86.

[1] Lei YG, He YL, Li R, Gao YF. Effects of baffle inclination angle on flow and heat transfer of a heat exchanger with helical baffles. Chemical Engineering and Processing: Process Intensification. 2008;47(12):2336–2345.

[2] Li Z, Gao Y. Numerical study of turbulent flow and heat transfer in cross-corrugated triangular ducts with delta-shaped baffles. International Journal of Heat and Mass Transfer. 2017;108:658–670.

[3] Sriromreun P. Numerical study on heat transfer enhancement in a rectangular duct with incline shaped baffles. Chemical Engineering Transactions. 2017;57:1243–1248.

[4] Rashidi S, Eskandarian M, Mahian O, Poncet SJ. Combination of nanofluid and inserts for heat transfer enhancement: gaps and challenges. Journal of Thermal Analysis and Calorimetry. 2019;135:437–460.

[5] Alnak DE. Thermohydraulic performance study of different square baffle angles in cross-corrugated channel. Journal of Energy Storage. 2020;28:101295.

[6] Chang SW, Cheng TH. Thermal performance of channel flow with detached and attached pin-fins of hybrid shapes under inlet flow pulsation. International Journal of Heat and Mass Transfer. 2021;164:120554.

[7] Keklikcioglu O, Ozceyhan V. Experimental investigation on heat transfer enhancement of a tube with coiled-wire inserts installed with a separation from the tube wall. International Communications in Heat and Mass Transfer. 2016;78:88–94.

[8] Nanan K, Piriyarungrod N, Thianpong C, Wongcharee K, Eiamsa-ard S. Numerical and experimental investigations of heat transfer enhancement in circular tubes with transverse twisted-baffles. Heat and Mass Transfer. 2016;52:2177–2192.

[9] Ji J, Pan Y, Zhang J, Shi B, Bao L. Numerical study on the effect of baffle structure on the heat transfer performance of elastic tube bundle heat exchanger. Applied Thermal Engineering. 2024;238:122220.

[10] Al-darraji AR, Marzouk SA, Aljabr A, Almehmadi FA, Alqaed S, Kaood A. Enhancement of heat transfer in a vertical shell and tube heat exchanger using air injection and new baffles: experimental and numerical approach. Applied Thermal Engineering. 2024;236:121493.

[11] Bhattacharyya S, Sharma AK, Vishwakarma DK, Goel V, Paul AR. Influence of magnetic baffle and magnetic nanofluid on heat transfer in a wavy minichannel. Sustainable Energy Technologies and Assessments. 2023;56:102954.
[12] Bichkar P, Dandgaval O, Dalvi P, Godase R, Dey T. Study of shell and tube heat exchanger with the effect of types of baffles. Procedia Manufacturing. 2018;20:195–200.
[13] Menni Y, Chamkha AJ, Zidani C, Benyoucef B. Numerical analysis of heat and nanofluid mass transfer in a channel with detached and attached baffle plates. Mathematical Modelling of Engineering Problems. 2019;6(1).
[14] Nithya M, Vel MS, Anitha S, Sivaraj C. Optimizing thermal efficiency: advancements in flat plate heat exchanger performance through baffle integration. International Communications in Heat and Mass Transfer. 2024;158:107885.
[15] Akçay S. Numerical analysis of hydraulic and thermal performance of Al_2O_3-water nanofluid in a zigzag channel with central winglets. Gazi University Journal of Science. 2023;36(1):383–397.
[16] De D, Pal TK, Bandyopadhyay S. Helical baffle design in shell and tube type heat exchanger with CFD analysis. International Journal of Heat and Technology. 2017;35(2):378–383.
[17] Lima-Téllez T, Hinojosa JF, Hernández-López I, Moreno S. Numerical study of the thermal performance of a single-channel cooling PV system using baffles and different nanofluids. Heliyon. 2024;10(15).
[18] Reddy PN, Verma V, Kumar A, Awasthi MK. CFD simulation and thermal performance optimization of channel flow with multiple baffles. Journal of Heat and Mass Transfer Research. 2023;10(2):257–268.
[19] Ali SA, Rasheed SA. Effect of partially filled porous media on laminar flow and heat transfer via forced convection of fluid flow within a channel at different angles: a numerical study. AIP Conference Proceedings. 2025;3169(1).
[20] Ali SA, Barrak ES, Alrikaby NJ, Hameed MR. Numerical study of thermal-hydraulic performance of forced convection heat transfer in dimple surface pipe with different shapes using commercial CFD code. Heat Transfer. 2025;125(2):1–5.
[21] Aljabair S, Mohammed AA, Alesbe I. Natural convection heat transfer in corrugated annuli with H_2O–Al_2O_3 nanofluid. Heliyon. 2020;6(11).
[22] Karamallah AA, Mahmoud NS. Experimental investigation of heat transfer enhancement with nanofluid and twisted tape inserts in a circular tube. Engineering and Technology Journal. 2016;34(3A):664–684.
[23] Elfaghi AM, Abosbaia AA, Alkbir MF, Omran AA. Heat transfer enhancement in pipe using Al_2O_3/water nanofluid. CFD Letters. 2022;14(9):118–124.
[24] Elfaghi AM, Mustaffa M. Numerical simulation of forced convection heat transfer in pipe using different nanoparticles. Journal of Complex Flow. 2021;3(2):33–37.
[25] Abobaker M, Addeep S, Afolabi LO, Elfaghi AM. Effect of mesh type on numerical computation of aerodynamic coefficients of NACA 0012 airfoil. Journal of Advanced Research in Fluid Mechanics and Thermal Sciences. 2021;87(3):31–39.
[26] Hameed MR, Al Sarmad Ahmed A, Hadwan HH, Toman AA, Mahdi MA. CFD-FSI analysis of textured journal bearing working with nano lubricant. Diagnostyka. 2024;25(2).
[27] Togun H, Homod RZ, Aljibori HS, Abed AM, Alias H, Hussein AK, Biswal U, Al-Thamir M, Mahdi JM, Mohammed HI, Ahmadi G. Al_2O_3–Cu hybrid nanofluid flow and heat transfer characteristics in the duct with various triangular rib configurations. Journal of Thermal Analysis and Calorimetry. 2024;149(17):10047–10060.
[28] Shojaee S, Vahabi M, Dinarvand S, Hamedi A, Mirabdolah Lavasani A, Moinfar Z. Twisted-tape inserts of rectangular and triangular sections in turbulent flow of CMC/CuO non-Newtonian nanofluid into an oval tube. International Journal of Numerical Methods for Heat & Fluid Flow. 2024;34(12):4535–4564.
[29] Marzouk SA, Almehmadi FA, Aljabr A, Sharaf MA. Numerical and experimental investigation of heat transfer enhancement in double tube heat exchanger using nail rod inserts. Scientific Reports. 2024;14(1):9637.
[30] Ali SA. Influence of inserted different ribs configuration in 2D horizontal channel on characteristics turbulent fluid flow and forced heat transfer: a numerical investigation. Journal of Research and Applications in Mechanical Engineering. 2025;13(1).
[31] Blazek J. Computational fluid dynamics: principles and applications. Butterworth-Heinemann; 2015.
[32] Rebollo TC, Lewandowski R. Mathematical and numerical foundations of turbulence models and applications. Springer New York; 2014.
[33] Zhang L, Che D. Influence of corrugation profile on the thermal-hydraulic performance of cross-corrugated plates. Numerical Heat Transfer, Part A: Applications. 2011;59(4):267–296.

[34] Anjaneya G, Sunil S, Manjunatha NK, Santhosh A, Patil SA, Prasad CD, Aden AA, Giriswamy BG. Study of impact of nanofluids on performance of microchannel heat exchangers using CFD. International Journal of Thermofluids. 2024;24:100836.
[35] Abumandour RM, El-Reafay AM, Salem KM, Dawood AS. Numerical investigation by cut-cell approach for turbulent flow through an expanded wall channel. Axioms. 2023;12(5):442.
[36] Abumandour RM, El-Reafay AM, Salem KM, Dawood AS. Numerical investigation by cut-cell approach for turbulent flow through an expanded wall channel. Axioms. 2023;12(5):442.
[37] Yuan W, Zhang X, Poirel D. Numerical investigation of aerodynamic response to gust including gust-induced dynamic stall. AIAA Aviation Forum and Ascend. 2024:4475.